An optimized-effective-potential method for solids with exact exchange and random-phase approximation correlation

1998 J. Phys.: Condens. Matter 10 9241

(http://iopscience.iop.org/0953-8984/10/41/007)

J. Phys.: Condens. Matter **10** (1998) 9241–9261. Printed in the UK PII: S0953-8984(98)95950-1

An optimized-effective-potential method for solids with exact exchange and random-phase approximation correlation

Takao Kotani

Department of Physics, Osaka University, Toyonaka 560, Japan

Received 15 July 1998

Abstract. We present a new density-functional method which does not exploit the local density approximation (LDA). In this method, we use an exchange–correlation energy which consists of the exact exchange (EXX) energy and the correlation energy in the random-phase approximation (RPA). A static approximation is used in the evaluation of the functional derivative of the RPA correlation energy. The self-consistent results for solid Cu, Fe, Co, Ni, Si, and MnO (type-II antiferromagnets) are presented. For the transition metals Cu, Fe, Co, and Ni, it is shown that the correlation potential gives rise to a large contribution which has the opposite sign to the exchange potential. The resulting eigenvalue dispersions and the magnetic moments are very close to those of the LDA and experiments. On the other hand, the Fermi-contact parts of the hyperfine field are rather different from the LDA results, and are in better agreement with experiments. The band gap obtained for Si is larger than the LDA value by ∼0.2 eV. For MnO, the density of states shows good correspondence with data obtained by x-ray photoelectron spectroscopy and bremsstrahlung isochromat spectroscopy.

1. Introduction

The optimized-effective-potential (OEP) method for electronic structure calculations was first applied to atoms by Talman and Shadwick [1], who introduced it as a method of restricted minimization of the Hartree–Fock (HF) total energy. In that method, they restricted the one-particle potential to a local potential instead of the non-local HF potential. From the viewpoint of the density-functional (DF) formalism, their calculations are considered as the DF calculation with the Kohn–Sham (KS) exact exchange (EXX) without the correlation. In recent years, we have extended the method so that it is now applicable also for solids [2–5]. In this form of the method, we take account of the correlation energy in the framework of the local density approximation (LDA). On the other hand, Krieger, Li, and Iafrate (KLI) [6, 7] developed a different type of approximation for the EXX potential. It was applied to Si and Ge by Bylander and Kleinman in the framework of the pseudopotential method [8]. Recently, Städele *et al* [9] developed the EXX method without using the KLI approximation within the pseudopotential theory. They applied the method to a series of semiconductors.

As was shown in the above studies, despite of the potentiality of the EXX method for going beyond the LDA, the results were not always satisfactory. In particular, for transition metals such as Fe [3], the method predicted occupied d bands which were too deep relative to the s bands and also gave rise to too large magnetizations. This indicates that the LDA correlation is not suitable for combining with EXX, and that the correlation consistent with EXX should give rather large contributions cancelling the EXX contribution.

0953-8984/98/419241+21$19.50

There are some possible ways of taking into account the correlation energy more rigorously. Here we select the method that is based on the DF theory. In this method, the DF correlation energy is calculated with the KS orbitals. Our exchange–correlation (XC) energy consists of the EXX energy and a correlation energy obtained in the random-phase approximation (RPA). In section 2, we derive the OEP method as a restricted variational form of the self-consistent GW-method. The static approximation used for the functional derivative of the RPA correlation energy with respect to the density is explained. In section 3, we explain how to implement the OEP method in the atomic sphere approximation (ASA). A static screened Coulomb interaction, which is used for the evaluation of the RPA correlation, is calculated by use of the product-basis method developed by Aryasetiawan and Gunnarsson [11]. In section 4, we give the results obtained for some typical systems. For the transition metals Fe, Co, Ni, and Cu, it gives rather good agreement with the LDA. For Si, the band gap obtained is larger than that given by the LDA by ∼0.2 eV. It is consistent with a previous evaluation by Godby, Shlüter, and Sham [12]. For MnO, the result lies in between the LDA and EXX results, and shows reasonable correspondence with data obtained by x-ray photoelectron spectroscopy and bremsstrahlung isochromat spectroscopy (XPS + BIS data) [13].

2. Formalism

2.1. The self-consistent GW-method versus the OEP method

First, we review the so-called self-consistent GW-method (the SCGW method). The SCGW equation is derived by minimizing the total energy $E[G]$ which is a functional of the Green function G; it was originally introduced by Luttinger and Ward [14]. The Hamiltonian of a system of electrons is written as

$$\hat{H} = \sum_{\sigma} \int \mathrm{d}\boldsymbol{r}\ \hat{\psi}^{\dagger}_{\sigma}(\boldsymbol{r})\left(-\frac{\nabla^2}{2m}\right)\hat{\psi}_{\sigma}(\boldsymbol{r}) + \hat{V}_{ee} + \sum_{\sigma}\int \mathrm{d}\boldsymbol{r}\ (v^{\mathrm{ext}}_{\sigma}(\boldsymbol{r}) - \mu)\hat{n}_{\sigma}(\boldsymbol{r}) \tag{1}$$

where

$$\hat{V}_{ee} = \frac{\lambda e^2}{2}\sum_{\sigma\sigma'}\int \mathrm{d}\boldsymbol{r}\ \mathrm{d}\boldsymbol{r}'\ \frac{\hat{\psi}^{\dagger}_{\sigma}(\boldsymbol{r})\hat{\psi}^{\dagger}_{\sigma'}(\boldsymbol{r}')\hat{\psi}_{\sigma'}(\boldsymbol{r}')\hat{\psi}_{\sigma}(\boldsymbol{r})}{|\boldsymbol{r}-\boldsymbol{r}'|} \tag{2}$$
$$\hat{n}_{\sigma}(\boldsymbol{r}) = \hat{\psi}^{\dagger}_{\sigma}(\boldsymbol{r})\hat{\psi}_{\sigma}(\boldsymbol{r})$$

where we use the usual notation for the field operators $\hat{\psi}_{\sigma}(\boldsymbol{r})$, chemical potential μ, spin index σ, and external potential $v^{\mathrm{ext}}_{\sigma}(\boldsymbol{r})$. The parameter λ is set to unity (it is later used as an integration variable). Let us start from $W[J]$, defined by

$$\exp(W[J]) = \mathrm{Tr}\left[T\exp\left\{-\int_0^{\beta}\mathrm{d}\tau\ \hat{H} + \int \mathrm{d}1\int \mathrm{d}2\ \hat{\psi}^{\dagger}_{\sigma_1}(\boldsymbol{r}_1)J(1,2)\hat{\psi}_{\sigma_2}(\boldsymbol{r}_2)\right\}\right] \tag{3}$$

where we use the notation $1 \equiv \boldsymbol{r}_1\sigma_1\tau_1$ $(0 \leqslant \tau \leqslant \beta)$. T stands for imaginary-time ordering, and $J(1,2)$ is a source term. $W[J]$ is a finite-temperature generating functional for the Green functions; its nth derivative with respect to $J(1,2)$ gives the n-body Green function. The first derivative of $W[J]$ gives

$$\frac{\delta W[J]}{\delta J(1,2)} = -\langle T\hat{\psi}(2)\hat{\psi}^{\dagger}(1)\rangle_J \equiv -G(2,1). \tag{4}$$

The bracket $\langle\cdots\rangle_J$ denotes thermal averaging for a fixed external source field J. When we set $J=0$, G equals the Green function for the system. The effective action $\Gamma[G]$ is defined as the Legendre transform of $W[J]$:

$$\Gamma[G] = -W[J] + \int \mathrm{d}1 \int \mathrm{d}2\ J(1,2)\frac{\delta W[J]}{\delta J(1,2)}. \tag{5}$$

Here J should be treated as a functional of G. If we assume that $\det(\delta G/\delta J|_{J=J_\mathrm{A}}) \neq 0$, J as a functional of G can be defined at least in the neighbourhood of $J=J_\mathrm{A}$. Also $\Gamma[G]$ is well defined there. Then we can easily see that

$$\frac{\delta\Gamma[G]}{\delta G(2,1)} = -J(1,2). \tag{6}$$

We can separate the functional $\Gamma[G]$ into the kinetic, external, Coulomb, and XC terms, following the coupling-integral method given in references [15–17]. Let us consider the generating functional $W_\lambda[J]$, which is for the system with the coupling constant λe^2 $(0 \leqslant \lambda \leqslant 1)$. For each λ, J_λ is fixed so as to generate the given $G(2,1)$; that is,

$$\frac{\delta W_\lambda[J_\lambda]}{\delta J_\lambda(1,2)} = -G(2,1). \tag{7}$$

Note that we now consider G as the quantity of the zeroth order in λe^2. The derivative $\mathrm{d}W_\lambda[J_\lambda]/\mathrm{d}\lambda$ can be written as

$$\frac{\mathrm{d}W_\lambda[J_\lambda]}{\mathrm{d}\lambda} = -\int_0^\beta \mathrm{d}\tau\ \langle\hat{V}_{ee}(\tau)\rangle_{G,\lambda} - \int \mathrm{d}1 \int \mathrm{d}2\ G(2,1)\frac{\mathrm{d}J_\lambda(1,2)}{\mathrm{d}\lambda}. \tag{8}$$

The subscripts G and λ indicate functionals of G and λ. Through the integration of equation (8) with respect to λ, we can write $\Gamma[G]$ as

$$\Gamma[G] = \Gamma_{\lambda=0}[G] + \frac{e^2}{2}\sum_{\sigma,\sigma'}\int_0^\beta \mathrm{d}\tau \int \mathrm{d}\boldsymbol{r}_1\ \mathrm{d}\boldsymbol{r}_2\ \frac{n_\sigma(\boldsymbol{r}_1,\tau)n_{\sigma'}(\boldsymbol{r}_2,\tau)}{|\boldsymbol{r}_1-\boldsymbol{r}_2|} + \Gamma_\mathrm{xc}[G] \tag{9}$$

$$\Gamma_\mathrm{xc}[G] = \frac{e^2}{2}\sum_{\sigma,\sigma'}\int_0^1 \mathrm{d}\lambda \int_0^\beta \mathrm{d}\tau \int \mathrm{d}\boldsymbol{r}_1\ \mathrm{d}\boldsymbol{r}_2 \left(\frac{\langle\hat{\psi}^\dagger_\sigma(\boldsymbol{r}_1,\tau)\hat{\psi}^\dagger_{\sigma'}(\boldsymbol{r}_2,\tau)\hat{\psi}_{\sigma'}(\boldsymbol{r}_2,\tau)\hat{\psi}_\sigma(\boldsymbol{r}_1,\tau)\rangle_{G,\lambda}}{|\boldsymbol{r}_1-\boldsymbol{r}_2|} - \frac{n_\sigma(\boldsymbol{r}_1,\tau)n_{\sigma'}(\boldsymbol{r}_2,\tau)}{|\boldsymbol{r}_1-\boldsymbol{r}_2|}\right) \tag{10}$$

where

$$n_\sigma(\boldsymbol{r}_1,\tau) \equiv G(\boldsymbol{r}_1\sigma\tau, \boldsymbol{r}_1\sigma\tau^+). \tag{11}$$

$\Gamma_{\lambda=0}[G]$ is the kinetic + external energy functional (non-interacting part) defined as the Legendre transform of $W_{\lambda=0}[G]$. The second term on the right-hand side (r.h.s.) of equation (9) corresponds to the Coulomb term, and the third to the XC term as the functional of $G(1,2)$. The diagrammatical rules for the evaluation of $\Gamma_\mathrm{xc}[G]$ are rather straightforward [18]. Hereafter we consider the zero-temperature limit in the case where $J(1,2)$ depends only on $\tau_1-\tau_2$. Then $\Gamma[G]$ can be reduced to the energy in the real-time formalism:

$$E[G] = E_\mathrm{k}[G] + E_\mathrm{ext}[G] + E_\mathrm{Cou}[G] + E_\mathrm{xc}[G].$$

$\delta E[G]/\delta G = 0$, corresponding to equation (6), determines the real-time Green function G. It can be separated into a pair of equations:

$$\frac{\delta E_\mathrm{k}}{\delta G(1,2)} + V^\mathrm{eff}(1,2) = 0 \tag{12}$$

$$V^\mathrm{eff}(1,2) = \{V_\mathrm{Cou}(\boldsymbol{r}_1) + V_\mathrm{ext}(\boldsymbol{r}_1)\}\delta(1-2) + \Sigma(1,2) \tag{13}$$

where we have introduced the one-particle effective potential $V^{\rm eff}(1,2)$, and the self-energy $\Sigma(1,2)$, defined as $\Sigma(1,2)[G] \equiv \delta E_{\rm xc}[G]/\delta G$.

In the RPA, $E_{\rm xc}^{\rm RPA}[G] = E_{\rm x}[G] + E_{\rm c}^{\rm RPA}[G]$ is written as

$$E_{\rm x}[G] = -\frac{e^2}{2}\sum_\sigma \int\int \frac{n_\sigma(\boldsymbol{r},\boldsymbol{r}')n_\sigma(\boldsymbol{r}',\boldsymbol{r})}{|\boldsymbol{r}-\boldsymbol{r}'|}\,{\rm d}\boldsymbol{r}\,{\rm d}\boldsymbol{r}' \tag{14}$$

$$E_{\rm c}^{\rm RPA}[G] = \frac{\rm i}{2}\int_0^1 \frac{{\rm d}\lambda}{\lambda}\,{\rm Tr}[(1-v_\lambda D)^{-1}v_\lambda D - v_\lambda D] = \frac{-\rm i}{2}\,{\rm Tr}[\log(1-vD)+vD] \tag{15}$$

where the trace applies to $\boldsymbol{r}\sigma t$ (I suppress the factor $1/\int_{-\infty}^{\infty}{\rm d}t$ for simplicity), $n_\sigma(\boldsymbol{r},\boldsymbol{r}') \equiv -{\rm i}G(\boldsymbol{r}\sigma t, \boldsymbol{r}'\sigma t^+)$, and $D(1,2) \equiv -{\rm i}G(1,2)G(2,1)$. v_λ is defined as

$$v_\lambda(1,2) = \lambda e^2\delta(t_1-t_2)\delta_{\sigma_1\sigma_2}/|\boldsymbol{r}_1-\boldsymbol{r}_2|.$$

v denotes $v_{\lambda=1}$. The SCGW equation can be obtained if we use $\Sigma^{\rm RPA}(1,2)[G]$, which is defined as the functional derivative of $E_{\rm xc}^{\rm RPA}[G]$, in equation (13).

However, it is rather difficult to solve the SCGW equation. As a substitution in the SCGW equation, we take $E[G^0]$ instead of $E[G]$; G^0 means the Green function which is generated from the local and ω-independent one-particle effective potential. This means that we consider the optimum solution under such a constraint. This is nothing but the OEP method. We restrict ourselves to the spin-diagonal case. For a given one-particle effective potential $V_\sigma^{\rm eff}(\boldsymbol{r})$, G^0 is expressed as ($\delta \to +0$)

$$G_\sigma^0(\boldsymbol{r}_1,\boldsymbol{r}_2,\omega) = \sum_i \frac{\psi_\sigma^{i*}(\boldsymbol{r}_1)\psi_\sigma^i(\boldsymbol{r}_2)}{\omega-\epsilon_\sigma^i+{\rm i}\delta\,{\rm sgn}(\epsilon_\sigma^i)} \tag{16}$$

where ϵ_σ^i and ψ_σ^i are the eigenvalues and eigenfunctions satisfying

$$[-\nabla^2/(2m) + V_\sigma^{\rm eff}(\boldsymbol{r}) - \epsilon_\sigma^i]\psi_\sigma^i(\boldsymbol{r}) = 0.$$

Then the minimization equation

$$0 = \int {\rm d}1\ {\rm d}2\ \frac{\delta E[G^0]}{\delta G^0(1,2)}\frac{\delta G^0(1,2)}{\delta V_\sigma^{\rm eff}(\boldsymbol{r})} \tag{17}$$

reduces to

$$\frac{\delta E_{\rm k}}{\delta G^0(1,2)} + V_{\sigma_1}^{\rm eff}(\boldsymbol{r}_1)\delta(1-2) = 0 \tag{18}$$

$$V_{\sigma_1}^{\rm eff}(\boldsymbol{r}_1) \equiv V^{\rm Cou}(\boldsymbol{r}_1) + V^{\rm ext}(\boldsymbol{r}_1) + V_{\sigma_1}^{\rm xc}(\boldsymbol{r}_1) \tag{19}$$

$$\int {\rm d}1\ {\rm d}2\ \left[V_{\sigma_1}^{\rm xc}(\boldsymbol{r}_1)\delta(1-2) - \Sigma^{\rm RPA}(1,2;G^0)\right]\frac{\delta G^0(1,2)}{\delta V_\sigma^{\rm eff}(\boldsymbol{r})} = 0. \tag{20}$$

Equation (18) is the ordinary equation used to determine the non-interacting one-body Green function for $V^{\rm eff}$. Equation (20), which determines $V^{\rm xc}$, is rewritten as

$$\frac{\delta E_{\rm xc}^{\rm RPA}}{\delta V_\sigma^{\rm eff}(\boldsymbol{r})} = \int {\rm d}^3r'\ \frac{\delta n_\sigma(\boldsymbol{r}')}{\delta V_\sigma^{\rm eff}(\boldsymbol{r})}V_\sigma^{\rm xc}(\boldsymbol{r}'). \tag{21}$$

Note that the matrix $\delta n_\sigma(\boldsymbol{r}')/\delta V_\sigma^{\rm eff}(\boldsymbol{r})$ is spin diagonal because $V^{\rm eff}$ includes the chemical potential.

Our variational parameter is $V^{\rm eff}$; therefore, we can consider our method (relying on the one-to-one correspondence between $V_\sigma^{\rm eff}(\boldsymbol{r})$ and $n_\sigma(\boldsymbol{r})$) as a DF method. Then $V_\sigma^{\rm xc}(\boldsymbol{r})$ is identified as $\delta E_{\rm xc}^{\rm RPA}/\delta n_\sigma(\boldsymbol{r})$. The only difference from the ordinary LDA calculation is that

$V^{\rm xc}$ is calculated following equation (21). In the definition of $E_{\rm xc}^{\rm RPA}$ using equations (14)–(15), we use G^0 and $D^0(1,2) \equiv -{\rm i}G^0(1,2)G^0(2,1)$, instead of G and $D(1,2)$. $D^0(1,2)$ is written as

$$D_\sigma^0(\boldsymbol{r}_1,\boldsymbol{r}_2,\omega) = \sum_i^{\rm occ}\sum_j^{\rm unocc} \psi_\sigma^{i*}(\boldsymbol{r}_1)\psi_\sigma^i(\boldsymbol{r}_2)\psi_\sigma^{j*}(\boldsymbol{r}_2)\psi_\sigma^j(\boldsymbol{r}_1) \times \left\{\frac{1}{\omega-\epsilon_\sigma^j+\epsilon_\sigma^i+{\rm i}\delta} - \frac{1}{\omega+\epsilon_\sigma^j-\epsilon_\sigma^i-{\rm i}\delta}\right\}. \tag{22}$$

Such an OEP method at the RPA level has already been proposed by Gross, Dobson, and Petersilka in reference [19], where they discuss the relation of the OEP method to the Van der Waals interaction (we omit the term $f_{\rm xc}$ corresponding to the vertex correction).

In conclusion, the OEP method with EXX + RPA could be a starting point for the GW-approximation. As for the excitation energy, we can show that (minimum band gap) + (discontinuity in $V^{\rm xc}$) obtained by means of an OEP agrees with the minimum gap given by the GW-approximation (see appendix A).

2.2. The static approximation for the derivative of E_c^{RPA}

We use a static approximation in the evaluation of $\delta E_{\rm xc}^{\rm RPA}/\delta V_\sigma^{\rm eff}(\boldsymbol{r})$. The variation $\delta E_{\rm c}$ (we omit the superscript 'RPA' hereafter) with respect to δD^0 can be written as

$$\delta E_{\rm c} = \frac{\rm i}{2}\,{\rm Tr}[W_{\rm p}\,\delta D^0] \tag{23}$$

$$W_{\rm p} = v_{\rm sc} - v = v(1-vD^0)^{-1}v \tag{24}$$

where $v_{\rm sc} \equiv (1-vD^0)^{-1}v$ denotes the dynamical screened Coulomb interaction in the RPA. We evaluate $\delta E_{\rm c}$ in a static approximation, i.e., we replace $W_{\rm p}(\boldsymbol{r}_1,\boldsymbol{r}_2,t_1-t_2)$ with $W_{\rm p}^{\omega=0}(\boldsymbol{r}_1,\boldsymbol{r}_2)\delta(t_1-t_2)$, where we define

$$W_{\rm p}^{\omega=0}(\boldsymbol{r}_1,\boldsymbol{r}_2) \equiv \int_{-\infty}^{\infty} {\rm d}t\ W_{\rm p}(\boldsymbol{r}_1,\boldsymbol{r}_2,t).$$

This approximation is justifiable if the relaxation time of the dynamical screening $v_{\rm sc}$, typically the plasma oscillation timescale, is sufficiently shorter than that of the density fluctuation ${\rm i}D^0$. We know that

$${\rm i}D_\sigma^0(\boldsymbol{r}_1,\boldsymbol{r}_2,t_1=t_2) = n_\sigma(\boldsymbol{r}_1)\delta(\boldsymbol{r}_1-\boldsymbol{r}_2) - [n_\sigma(\boldsymbol{r}_1,\boldsymbol{r}_2)]^2.$$

Here we use the non-local density

$$n_\sigma(\boldsymbol{r}_1,\boldsymbol{r}_2) \equiv \sum_i^{\rm occ} \psi_\sigma^{i*}(\boldsymbol{r}_1)\psi_\sigma^i(\boldsymbol{r}_2).$$

Then we obtain $\delta E_{\rm c} = \delta E_{\rm c1} + \delta E_{\rm c2}$, where we define

$$\delta E_{\rm c1} \equiv \frac{-1}{2}\sum_\sigma \int {\rm d}\boldsymbol{r}_1\ {\rm d}\boldsymbol{r}_2\ W_{\rm p}^{\omega=0}(\boldsymbol{r}_1,\boldsymbol{r}_2)\delta([n_\sigma(\boldsymbol{r}_1,\boldsymbol{r}_2)]^2) \tag{25}$$

$$\delta E_{\rm c2} \equiv \frac{1}{2}\sum_\sigma \int {\rm d}\boldsymbol{r}\ W_{\rm p}^{\omega=0}(\boldsymbol{r},\boldsymbol{r})\,\delta n_\sigma(\boldsymbol{r}). \tag{26}$$

$\delta E_{\rm c1}$ and $\delta E_{\rm c2}$ correspond to the correlated part of the screened exchange and the Coulomb-hole terms, respectively (see p 40 in reference [20]). As for $\delta E_{\rm c1}$, we can calculate its functional derivative $\delta E_{\rm c1}/\delta V_\sigma^{\rm eff}(\boldsymbol{r})$ from $W_{\rm p}^{\omega=0}(\boldsymbol{r}_1,\boldsymbol{r}_2)$, $n_\sigma(\boldsymbol{r}_1,\boldsymbol{r}_2)$, and $\delta n_\sigma(\boldsymbol{r}_1,\boldsymbol{r}_2)/\delta V_\sigma^{\rm eff}(\boldsymbol{r})$

through equation (25). We denote the resulting potential as $V_\sigma^{c1}(\boldsymbol{r}) = \delta E_{c1}/\delta n_\sigma(\boldsymbol{r})$. Obviously, we do not need the inversion of equation (21) for $\delta E_{c2}/\delta n_\sigma(\boldsymbol{r})$. $\delta E_{c2}/\delta n_\sigma(\boldsymbol{r})$ is spin independent and is written as $V_\sigma^{c2}(\boldsymbol{r}) = \frac{1}{2}W_p^{\omega=0}(\boldsymbol{r}, \boldsymbol{r})$. If we evaluate δE_c from equation (23) without using the static approximation, we obtain a result essentially equivalent to equation (27) in reference [12], which was used by Godby, Shlüter, and Sham to discuss the eigenvalues of the true density-functional theory. In section 4, we show that our result for Si is consistent with their result.

3. The OEP method in the LMTO-ASA

The OEP method with EXX + RPA is implemented within the ASA. First, we review the EXX method in the LMTO-ASA. Then we explain how to treat the RPA correlation within this scheme.

3.1. The LMTO-ASA and EXX

Any points in the space are denoted by $(\boldsymbol{r}, R)$, where R is the index for the atomic sphere (AS) and $\boldsymbol{r} = (r, \theta, \phi)$ is a vector denoting the position in each AS ($0 \leqslant r \leqslant \bar{R}$). In addition, we restrict ourselves to the spherical one-particle effective potential; that is, $V_\sigma^{\rm eff}(\boldsymbol{r})$ is replaced by $V_\sigma^{\rm eff}(r, R)$. Due to the one-to-one correspondence between $V_\sigma^{\rm eff}(r, R)$ and $n_\sigma^{\rm s}(r, R)$, we can consider $E_{\rm xc}$ as a functional of $n_\sigma^{\rm s}(r, R)$. Here $n_\sigma^{\rm s}(r, R)$ denotes the spherically averaged density.

In the LMTO method [21], the wave function $\psi^{\boldsymbol{k}j}(\boldsymbol{r}, R)$ with the energy $\epsilon^{\boldsymbol{k}j}$ is written as a linear combination of the localized MT orbitals (MTOs). The MTOs are constructed as linear combinations of the basis functions in each AS. The radial part $\phi_{Rl}(r)$ of the basis functions in each AS is determined by the radial Schrödinger equation (we use the units $\hbar = e^2/2 = 2m = 1$ hereafter) as

$$\left\{\frac{\mathrm{d}^2}{\mathrm{d}r^2} + \left[\epsilon_{\nu Rl} - \frac{l(l+1)}{r^2} - V^{\rm eff}(r, R)\right]\right\} r\phi_{Rl}(r) = 0. \tag{27}$$

$\epsilon_{\nu Rl}$ is determined in such a way that it is regular at $r = 0$, and its logarithmic derivative satisfies $D_{Rl} = \bar{R}\phi'_{Rl}/\phi_{Rl}|_{r=\bar{R}}$ at $r = \bar{R}$ (the overbar denotes the derivative with respect to r). With $\phi_{Rl}(r)$ and $\dot{\phi}_{Rl}(r)$ (the overdot denotes the energy derivative, and $\dot{\phi}_{Rl}(r)$ in this paper corresponds to $\dot{\phi}^{\gamma}_{Rl}(r)$ in reference [22]), we can express the wave function as

$$\psi^{\boldsymbol{k}j}(\boldsymbol{r}, R) = \sum_L \{A_{RL}^{\boldsymbol{k}j}\phi_{Rl}(r) + B_{RL}^{\boldsymbol{k}j}\dot{\phi}_{Rl}(r)\}Y_L(\theta, \phi) \tag{28}$$

where the Y_L are the real harmonics. To calculate $A_{RL}^{\boldsymbol{k}j}$ and $B_{RL}^{\boldsymbol{k}j}$ we need the LMTO Hamiltonian $H_{\rm MT}$ and the overlap integral $O_{\rm MT}$ for the MT potential. They are determined by the potential parameters $\mathcal{P}_{Rl} = (\epsilon_\nu, C, \sqrt{\Delta}, p, \gamma)_{Rl}$, which are also used to determine the coefficients for $\phi_{Rl}Y_L$ and $\dot{\phi}_{Rl}Y_L$ appearing in the MTOs.

The EXX energy $E_{\rm x}$ of equation (14) in the ASA can be evaluated through the procedure proposed by Svane and Andersen [23]. $E_{\rm x}$ for each spin (suppressing the spin index) for the valence electrons can be rewritten as

$$E_{\rm x} = -\sum W_{(R,R')}I_{RR'}(\widetilde{L}_1, \widetilde{L}_2, \widetilde{L}_3, \widetilde{L}_4)X^*_{R\widetilde{L}_3R'\widetilde{L}_2}X_{R\widetilde{L}_1R'\widetilde{L}_4} \tag{29}$$

$$X_{R\widetilde{L}_1R'\widetilde{L}_4} = \sum_{\boldsymbol{k}j}^{\rm occ} A^{\boldsymbol{k}j*}_{R\widetilde{L}_1}A^{\boldsymbol{k}j}_{R'\widetilde{L}_4}. \tag{30}$$

Here $\widetilde{L} = (L, I_{\rm P})$ is a composite index, where $I_{\rm P}$ takes the value 0 or 1: 0 corresponds to ϕ and 1 to $\dot{\phi}$; e.g., $A^{kj}_{R\widetilde{L}}$ denotes A^{kj}_{RL} and B^{kj}_{RL}. (R, R') and $W_{(R,R')}$ denote the non-equivalent pairs of the ASs and their weights. The summation of equation (29) is taken for (R, R'), $\widetilde{L}_1$, $\widetilde{L}_2$, $\widetilde{L}_3$, and $\widetilde{L}_4$. The quantity $I_{RR'}$ is defined as

$$I_{RR'}(\widetilde{L}_1, \widetilde{L}_2, \widetilde{L}_3, \widetilde{L}_4) = \int_R {\rm d}^3 r \int_{R'} {\rm d}^3 r' \; \frac{f^*_{R\widetilde{L}_1}(\boldsymbol{r}) f^*_{R'\widetilde{L}_2}(\boldsymbol{r}') f_{R\widetilde{L}_3}(\boldsymbol{r}) f_{R'\widetilde{L}_4}(\boldsymbol{r}')}{|(\boldsymbol{r}+\boldsymbol{R}) - (\boldsymbol{r}'+\boldsymbol{R}')|} \tag{31}$$

$$f_{R\widetilde{L}}(\boldsymbol{r}) = \phi_{R\widetilde{l}}(r) Y_L(\theta, \phi). \tag{32}$$

The contributions from the core–core and the core–valence parts to $E_{\rm x}$ can be included by extending the index $\widetilde{L}$ so that it runs over both $(L, I_{\rm P})$ and the index representing the core wave functions.

We can calculate $\delta E_{\rm x}/\delta V_{\rm eff}(r, R)$ by the use of a relation which is symbolically written as

$$\frac{\delta E_{\rm x}}{\delta V_{\rm eff}} = \left(\frac{\delta E_{\rm x}}{\delta X}\frac{\delta X}{\delta \mathcal{P}_{Rl}}\right)\frac{\delta \mathcal{P}_{Rl}}{\delta V_{\rm eff}} + \frac{\delta E_{\rm x}}{\delta I_{RR'}}\frac{\delta I_{RR'}}{\delta V_{\rm eff}}. \tag{33}$$

In order to calculate $\delta E_{\rm x}/\delta \mathcal{P}_{Rl}$ in the parentheses of the r.h.s., we use the simple two-point numerical derivative. Other quantities in the r.h.s. of equation (33) are calculated from $\phi_{R\widetilde{l}}(r)$ and $\delta\phi_{R\widetilde{l}}(r)/\delta V_{\rm eff}(r', R)$ in each AS. The latter quantity is expressed by the use of the two independent solutions of the radial Schrödinger equation, equation (27) [1] (and their energy derivatives). The logarithmic derivatives D_{Rl} are not the variational parameters, but are the quantities determined self-consistently in such a way that $\epsilon_{\nu Rl}$ is set equal to the centre of the gravity of the occupied states in the projected density of states (DOS). On the basis of an equation similar to equation (33), we can also calculate $\delta n_{\rm s}(r, R)/\delta V_{\rm eff}(r', R')$. Finally, we obtain $V^{\rm x}(r, R) = \delta E_{\rm x}/\delta n^{\rm s}(r, R)$ from the ASA version of equation (21):

$$\frac{\delta E_{\rm x}}{\delta V^{\rm eff}_\sigma(r, R)} = \sum_{R'} \int_0^{\tilde{R}'} {\rm d}r' \; \frac{\delta n^{\rm s}_\sigma(r', R')}{\delta V^{\rm eff}_\sigma(r, R)} V^{\rm x}_\sigma(r', R'). \tag{34}$$

Here, the summation with respect to R' is carried out only within the unit cell. We do not have to consider an impurity-like potential variation in the calculation of $\delta E_{\rm x}/\delta V_{\rm eff}(r, R)$ and $\delta n_{\rm s}(r', R')/\delta V_{\rm eff}(r, R)$. Instead, we take a variation $\delta V_{\rm eff}(r, R)$ preserving the crystal symmetry. The corresponding responses in $n_{\rm s}$ are then compatible with the crystal symmetry.

3.2. RPA correlation

In the evaluation of the functional derivative of the RPA correlation in the LMTO-ASA, we first have to calculate $W_{\rm p}^{\omega=0}$. This is done by extending the product-basis method proposed by Aryasetiawan and Gunnarsson [11]. The products of the radial functions are defined as

$$\widetilde{B}_i(\boldsymbol{r}) \equiv \phi_{\widetilde{R}n_1l_1}(r)\phi_{\widetilde{R}n_2l_2}(r) Y_L(\theta, \phi) \tag{35}$$

where $i = (\widetilde{R}, n_1l_1, n_2l_2, L)$, and l of L satisfies $|l_1 - l_2| \leqslant l \leqslant l_1 + l_2$ (we neglect products containing $\dot{\phi}$; see [11]). $\widetilde{R}$ denotes the AS in the primitive cell; thus $R = (\widetilde{R}, \boldsymbol{T})$. $\boldsymbol{T}$ denotes a crystal translation vector. Taking the Bloch sum of $\widetilde{B}_i(\boldsymbol{r})$ gives

$$\widetilde{B}_{\boldsymbol{k}i}(\boldsymbol{r}, \boldsymbol{T}) = {\rm e}^{{\rm i}\boldsymbol{k}\cdot\boldsymbol{T}}\widetilde{B}_i(\boldsymbol{r}). \tag{36}$$

D^0 and $D = D^0(1 - vD^0)^{-1}$ can be expanded into these Bloch bases. The matrix elements of D are written as ($\omega = 0$ is suppressed)

$$D(\boldsymbol{k}, i, j) = \langle B_{\boldsymbol{k}i}|D|B_{\boldsymbol{k}j}\rangle \tag{37}$$

where B_{kj} denotes the orthogonalized functions of $\widetilde{B}_{kj}$. Then we can expand $W_{\rm p} = vDv$ as

$$W_{\rm p}(\boldsymbol{r}, R, \boldsymbol{r}', R') = \sum_{\boldsymbol{k},s,t} C_{\boldsymbol{k}s}(\boldsymbol{r}, \boldsymbol{T}) W_{\rm p}(\boldsymbol{k}, s, t) C^*_{\boldsymbol{k}t}(\boldsymbol{r}', \boldsymbol{T}') \tag{38}$$

$$W_{\rm p}(\boldsymbol{k}, s, t) = \sum_{i,j} \langle C_{\boldsymbol{k}s}|v|B_{\boldsymbol{k}i}\rangle D(\boldsymbol{k}, i, j) \langle B_{\boldsymbol{k}j}|v|C_{\boldsymbol{k}t}\rangle \tag{39}$$

where new orthogonalized-basis functions $C_{\boldsymbol{k}t}$ are constructed from $\widetilde{C}_t(\boldsymbol{r}) = \{r\widetilde{B}_i(\boldsymbol{r}),\ r^n Y_L(\theta, \phi)\}$ in the same manner as was used for constructing $B_{\boldsymbol{k}j}$. Here n denotes an integer satisfying $0 \leqslant n \leqslant n_0^{\rm Max}$ (for $l = 0$), and $1 \leqslant n \leqslant n_l^{\rm Max}$ (for $l \geqslant 1$). In our previous paper [5], we used $B_{\boldsymbol{k}t}$ even for this expansion of $W_{\rm p}$. In that case, $V^{\rm c}$ in the vicinity of a nucleus was not so reliable because $\widetilde{B}_i(\boldsymbol{r})$ for the core states changes very rapidly when $\boldsymbol{r} \to 0$. For $\widetilde{C}_t(\boldsymbol{r})$, the rapid changes are suppressed by the factor r.

With this expansion for $W_{\rm p}^{\omega=0}$, we can evaluate $\delta E_{\rm c1}/\delta V_\sigma^{\rm eff}(r, R)$, in the same manner as equation (33), where we have to replace $I_{R,R'}$ by $J_{R,R'}$, which is defined with $W_{\rm p}^{\omega=0}(\boldsymbol{r}, R, \boldsymbol{r}', R')$ instead of $1/|(\boldsymbol{r} + \boldsymbol{R}) - (\boldsymbol{r}' + \boldsymbol{R}')|$ in equation (31). Therefore we can calculate $V_\sigma^{\rm c1}(r, R)$ by the inversion of equation (34) from $\delta E_{\rm c1}/\delta V_\sigma^{\rm eff}(r, R)$.

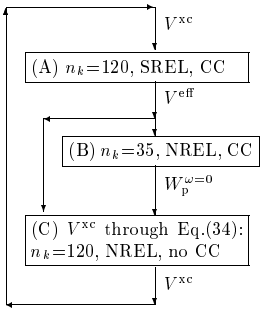

Figure 1. The self-consistency cycle for the EXX + RPA. n_k denotes the number of k-points in the IBZ (we show the n_k used in the case for metals). 'SREL' denotes the scalar-relativistic case. 'CC' denotes the combined correction [21].

We have developed a code to perform the self-consistent calculation for $V^{\rm c}$ together with $V^{\rm x}$. The flow chart of the self-consistent cycle is shown in figure 1.

There are three parts of the calculation:

(A) the self-consistent scalar-relativistic calculation with combined correction for a given $V^{\rm xc}$;

(B) the non-relativistic (NREL) calculation for obtaining $W_{\rm p}$ for a given $V^{\rm eff}$;

(C) the NREL calculation of $V^{\rm xc}$ with no combined correction for a given $V^{\rm eff}$ and $W_{\rm p}^{\omega=0}$.

Parts (B) and (C) are carried out to obtain $V^{\rm xc}$ for given $V^{\rm eff}$. Our calculation is based on the LMTO-4 code [24]. In the calculation of $W_{\rm p}$ of part (B), we have used a part of the GW-program [25, 26] provided by Aryasetiawan, though we use a tetrahedron method [27] in the calculation of D^0. Part (C) is developed from the LMTO-ASA EXX code used in reference [4]. The calculation is scalar relativistic with a non-relativistic $V^{\rm xc}$ (the previous results [2–5] were non-relativistic).

4. Results and discussion

We give the results of three different types of self-consistent calculation:

(i) those obtained using the OEP method with EXX and the RPA correlation, denoted by EXX + RPA;

(ii) those obtained using the OEP method with the EXX energy and the LDA correlation, denoted by EXX;

(iii) the results of usual LDA.

As the LDA correlation, we use the parametrization given by von Barth and Hedin [28]. This LDA gives the same total energy as the EXX + RPA in the case of the homogeneous electron gas.

4.1. Cu, Fe, Co, and Ni

We use the experimental lattice constants at zero temperature, 6.809, 5.406, 6.682, and 6.644 au [29] for Cu(fcc), Fe(bcc), Co(fcc), and Ni(fcc), respectively. For E_x and E_c, we take pairs (R, R') within up to the second-nearest neighbours and treat 4s, 4p, and 3d as valence orbitals. In procedure (B) of figure 1, the calculation of $W_p^{\omega=0}$, we use 35 k-points in the IBZ, and we use 120 k-points in parts (A) and (C). We use a minimum number of k-points for part (B) to reduce the computational work. We use product basis of 96 B_is, and 190 $\widetilde{C}_t$s. We omit the core eigenfunctions of 1s2s2p in the calculation of D_0 of equation (22).

In order to evaluate the numerical errors due to the cut-offs of the number of k-points and the number of the basis $\widetilde{C}_t$s, we have calculated the changes in the results occurring when we change these numbers (by carrying out the first iteration from the converged results). For Fe, we have done the calculations with 72 k-points for part (B) of figure 1 and the calculations for some different number of $\widetilde{C}_t$s. In addition, we have done the calculation including the 1s2s2p-core contributions to D_0. They indicate that the errors in all of the eigenvalues $\epsilon^{kj} - \mu$ are less than 0.01 eV.

In figure 2, we show the self-consistent $V^{xc} = V^x + V^{c1} + V^{c2}$. In our previous work, we were not able to determine the constant part included in V^{xc} because we calculated the functional derivatives $\delta E_x/\delta n_s(r)$ and so on under the constraint that the number of electrons is fixed [2–5]. In the present calculation, we calculate these derivatives without imposing such a constraint. This makes it possible to determine V^x and V^{c1} including their constant parts through the inversion of equation (34). The V^{xc} obtained by using the EXX + RPA are rather close to those obtained using the LDA. V^c shows a large difference between up and down spins and it almost cancels the contribution of V^x, which alone gives too large a magnetic moment [3].

The contribution of V^{c2} is largely cancelled by V^{c1} in the vicinity of the core region. This can be explained by the fact that $\delta n(\boldsymbol{r}_1, \boldsymbol{r}_2)$ is sufficiently short ranged for a given $\delta n(\boldsymbol{r})$ in this region, which allows us to evaluate δE_c approximately by use of $W_p^{\omega=0}(\boldsymbol{r}_1, \boldsymbol{r}_1)$ instead of $W_p^{\omega=0}(\boldsymbol{r}_1, \boldsymbol{r}_2)$ in equations (25) and (26). In this case, we have $\delta E_{c1} + \delta E_{c2} = 0$ because

$$\int \mathrm{d}\boldsymbol{r}_1 \; D_\sigma^0(\boldsymbol{r}_1, \boldsymbol{r}_2, t_1 = t_2) = 0.$$

On the other hand, we see a rather large cancellation between V^x and V^{c1} in the outer region ($r \gtrsim 1.0$ au). This is because the main contribution to δE_{c1} in equation (25) comes

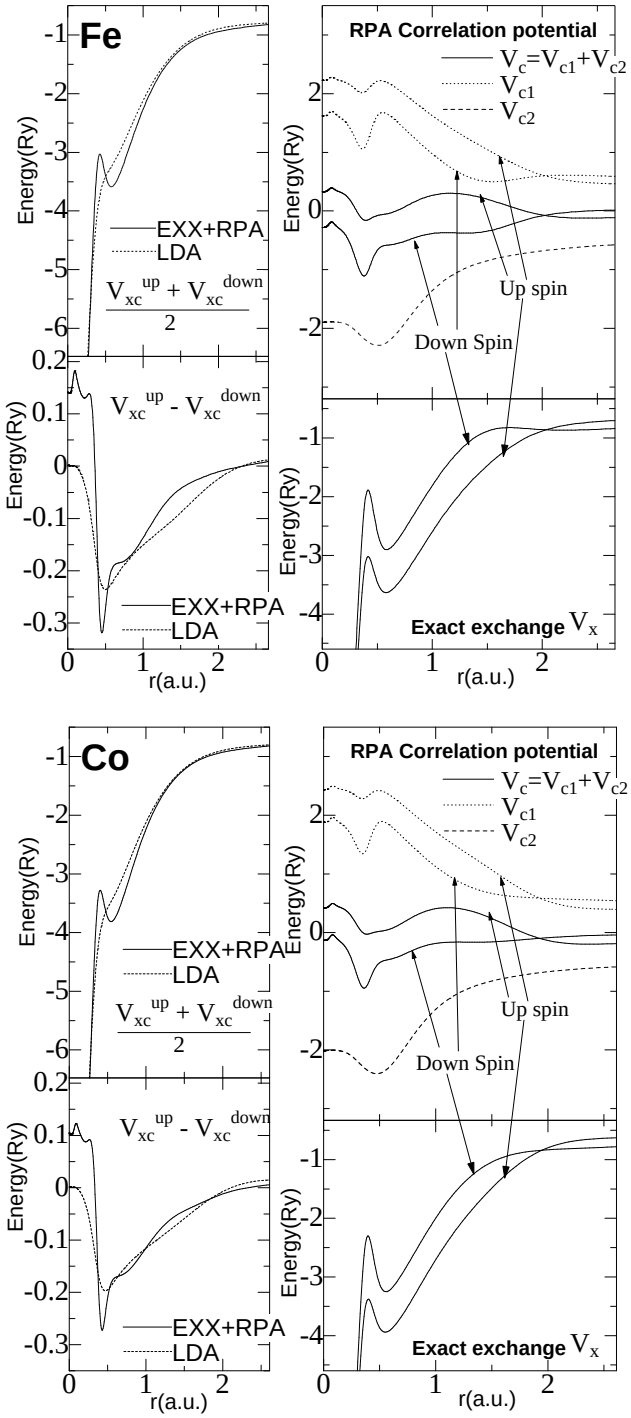

Figure 2. The exact exchange potential V^{x} and the RPA correlation potential $V^{\mathrm{c}} = V^{\mathrm{c1}} + V^{\mathrm{c2}}$ for Cu, Ni, Co, and Fe. The LDA XC potential [28], used as the reference, is calculated for the density determined by the self-consistent calculation using the EXX + RPA.

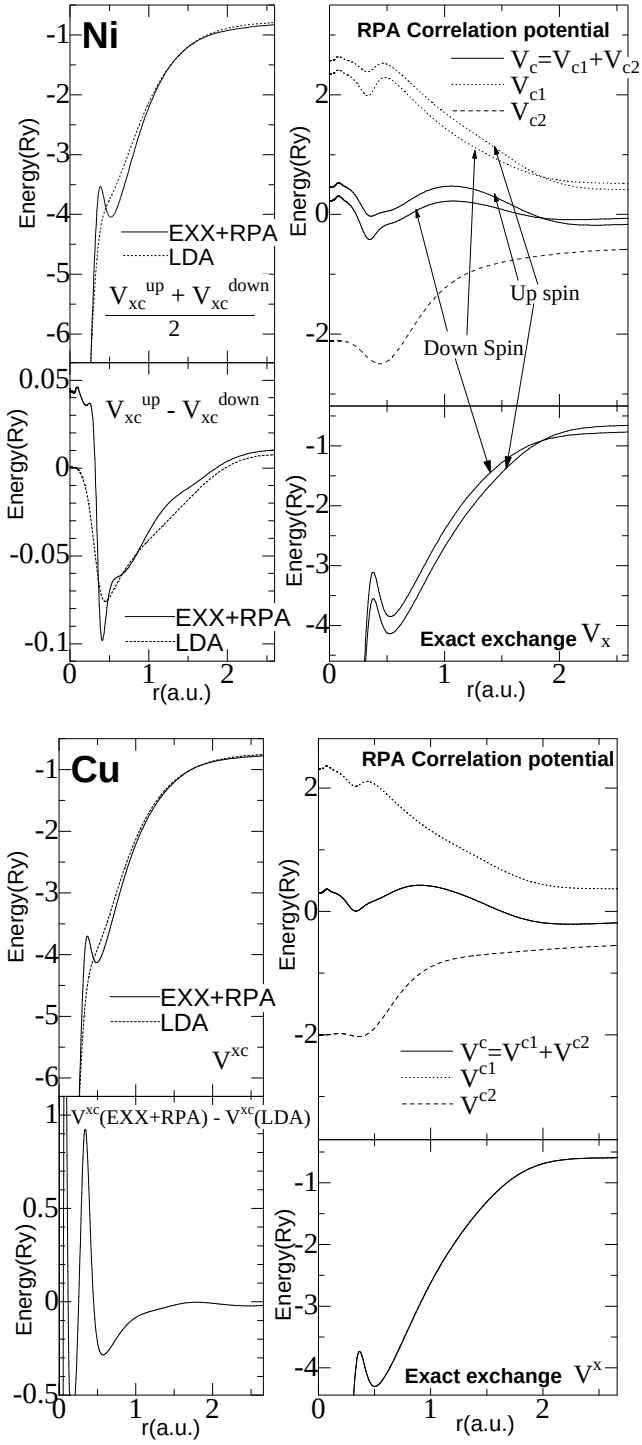

Figure 2. (Continued)

from the integral in the region $v_{sc}^{\omega=0} \sim 0$, where we expect the behaviour of $W_p^{\omega=0}$ to be as follows: $W_p^{\omega=0}(\boldsymbol{r}_1, \boldsymbol{r}_2) \sim -1/|\boldsymbol{r}_1 - \boldsymbol{r}_2|$.

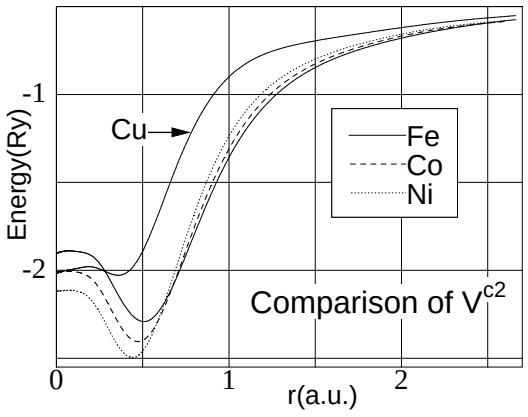

Figure 3. Comparison of V^{c2}.

V^{c2} itself has the meaning of a measure of the screening length: if we assume a simple form for the screening given by $v_{sc}^{\omega=0}(\boldsymbol{r}_1, \boldsymbol{r}_2) = \exp(-\kappa|\boldsymbol{r}_1 - \boldsymbol{r}_2|)/|\boldsymbol{r}_1 - \boldsymbol{r}_2|$, we can set $V^{c2} = -\kappa$ by definition. In figure 3, we replot V^{c2} for comparison. The V^{c2}s for Fe, Co, and Ni are very similar, though they are different from that of Cu, which is rather flat for $r \gtrsim 1.0$ au. Since we have little contribution from the 3d states to D^0 in equation (22) in the case of Cu, the difference indicates the effects of the screening by 3d electrons.

The eigenvalue dispersions are shown in figure 4 together with those calculated by using the usual LDA, and by using the EXX. The results obtained from the EXX + RPA are very close to those obtained by using the LDA, and are very different from the results obtained using EXX.

Table 1. Calculated spin magnetic moments (μ_B). We use the experimental lattice constants (see the text). The experimental spin magnetic moments are deduced from the saturation magnetization and the g-values [39]. In parentheses, we give the values for the lattice constants obtained using the LDA [40].

	LDA	EXX	EXX + RPA	Experiment
Fe	2.22(2.13)	3.40	2.05(2.00)	2.12
Co	1.59(1.54)	2.25	1.57(1.52)	1.59
Ni	0.61(0.58)	0.68	0.57(0.57)	0.56

In our method, we determine the screened Coulomb interaction $W_p^{\omega=0}$ and V^{eff} self-consistently at the same time. This makes the method applicable to a wide range of solids. However, our results for the energy bands in the present metallic systems are very close to the LDA results. This implies that it may not be necessary to determine $W_p^{\omega=0}$ self-consistently; that is, we are allowed to use the fixed $W_p^{\omega=0}$ calculated from the LDA eigenvalues (and eigenfunctions) during the self-consistent calculation. We have tried such a calculation for Fe, and obtained the magnetic moment 2.10 μ_B, which is close to the self-consistent value 2.05 μ_B given in table 1. Thus we can safely use $W_p^{\omega=0}$ from the LDA in most cases.

We show the calculated Fermi-contact parts of the hyperfine fields in table 2. They

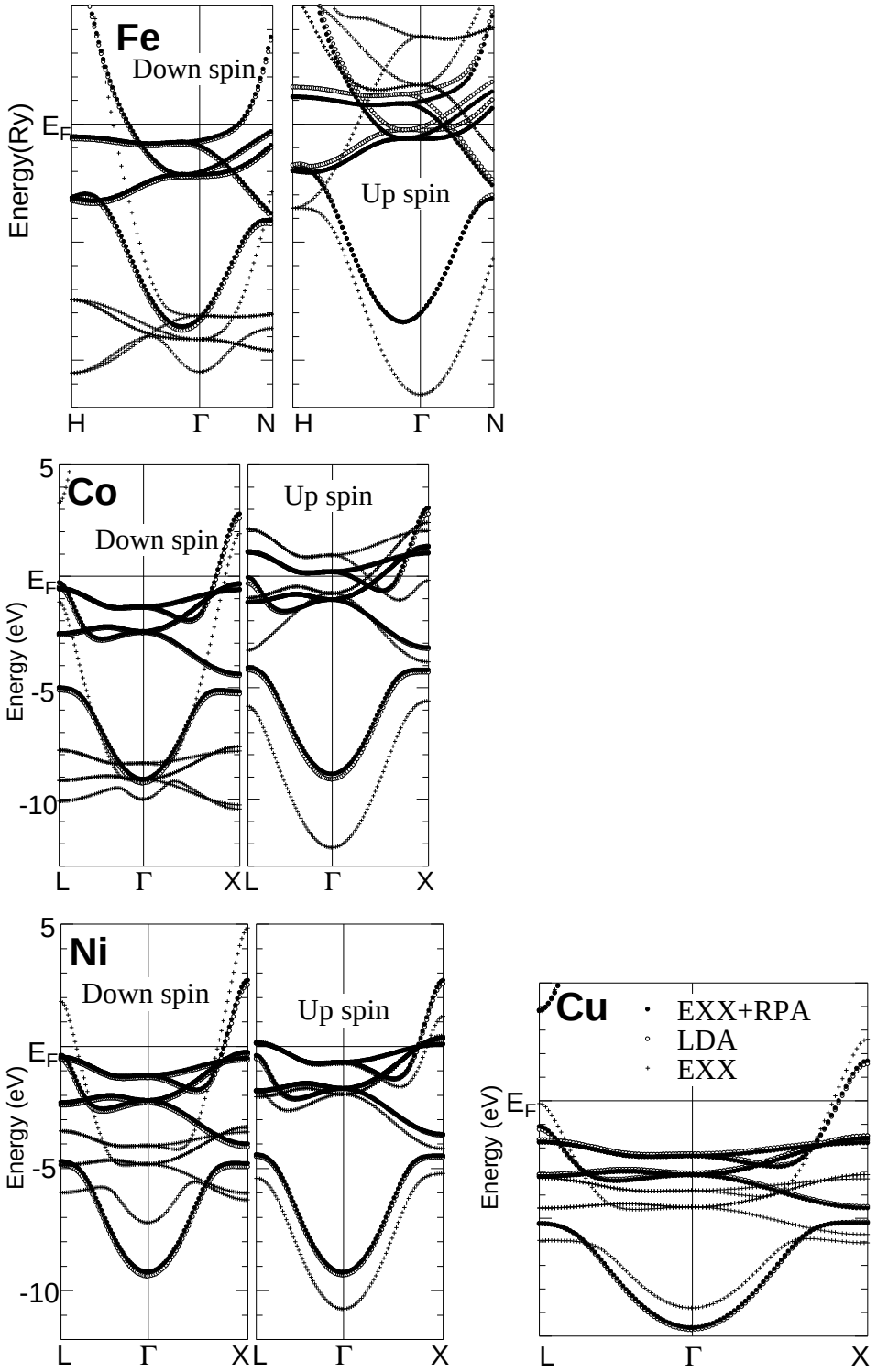

Figure 4. Energy bands obtained by performing three different types of self-consistent calculation: LDA, EXX, and EXX + RPA calculations. EXX denotes the calculation which is performed with the LDA correlation [28] potential plus the EXX potential.

Table 2. The Fermi-contact part of the hyperfine field (kG). The nuclear sizes are taken into account. The corresponding experimental data are taken from reference [31].

	Total	1s	2s	3s	4s (valence)
Fe					
EXX + RPA	−329	+ 86	−734	+ 370	−52
LDA	−279	−19	−516	+ 302	−46
Experiment	−375				
Co					
EXX + RPA	−323	+ 37	−635	+ 327	−52
LDA	−235	−17	−429	+ 267	−57
Experiment	−314				
Ni					
EXX + RPA	−135	+ 1	−251	+ 132	−17
LDA	−85	−8	−178	+ 114	−14
Experiment	−114				

are rather different from the LDA results. By the use of the self-consistently determined $V^{\rm xc}$, we calculate the hyperfine fields by means of the scalar-relativistic KKR-ASA code developed by Akai [30], where the wave function near the core is carefully treated and the core-size effects are taken into account [30]. The large positive parts of $V^{\rm xc}_{\uparrow} - V^{\rm xc}_{\downarrow}$ near the nucleus (figure 2) cause the strong negative polarization in the 2s state. In addition, our calculation shows positive polarization in the 1s state. This is different from the LDA result, which gives a negative polarization for the 1s state. We think that this comes from the strong 1s–2s and 1s–2p exchange interaction in the tail region of the 1s state. In order to gain the exchange energy, the 1s state should polarize negatively in the tail region, resulting in positive polarization near the nucleus. Our method can take into account the screened exchange effects in rather a reasonable way, whereas the LDA essentially fails in such a region where $\nabla n/n$ is very large [31]. The present method improves the agreement with experiments considerably.

4.2. Si and MnO

The lattice constant for Si is 8.40 au ($\bar{R}_{\rm Si} = \bar{R}_{\rm Es} = 2.526$ au) where Es denotes the empty spheres, and that for MnO (a type-II antiferromagnet) is assumed to be 10.26 au ($\bar{R}_{\rm Mn} = 2.923$ au and $\bar{R}_{\rm O} = 2.2$ au). For MnO and Si, we use a smaller number of $\widetilde{C}_t$s (e.g. 126 $\widetilde{C}_t$s for the Mn AS); we have checked that this is enough to reproduce the eigenvalues with an accuracy better than within 0.01 eV in the case of Fe. The numbers of k-points in the IBZ are, respectively, 19 and 29 in MnO and Si in all of the procedures ((A), (B), and (C) of figure 1). We take the pairs (R, R') within up to the second-nearest neighbours for Si, and within the first-nearest neighbours for MnO. In figure 2, we show the self-consistent $V^{\rm xc}$. The constant parts of $V^{\rm x}$ and $V^{\rm c1}$ are fixed arbitrarily for presentation purposes; they are not determined uniquely by our zero-temperature method in the case of insulators.

The eigenvalues of Si are shown in table 3. Using the EXX + RPA does not enlarge the band gaps very much from the LDA values. For example, the minimum gap increases by only 0.19 eV. The corresponding value given by Godby, Shlüter, and Sham in reference [12] was 0.14 eV. We can say that the agreement between these values is reasonable, considering

Table 3. Eigenvalues (in eV) for Si calculated by the EXX + RPA, by the EXX and by the LDA (scalar-relativistic) methods. They are given relative to the eigenvalue of $\Gamma_{25'v}$ (the top of the valence band). In addition, we show the results of the true DF calculation by Godby, Shlüter, and Sham.

	EXX	EXX + RPA	LDA	Godby *et al*[a]	Experiment[b]
Si					
$L_{2'v}$	−9.57	−9.75	−9.77		
L_{1v}	−6.86	−7.09	−7.15		
$L_{3'v}$	−1.13	−1.18	−1.20	−1.21(−1.22)	-1.2 ± 0.2, −1.5
L_{1c}	2.04	1.58	1.35	1.62(1.53)	2.1, 2.4 ± 0.15
L_{3c}	3.62	3.34	3.22	3.49(3.37)	4.15 ± 0.1
Γ_{1v}	−11.86	−12.08	−12.11		-12.5 ± 0.6
Γ_{15c}	3.05	2.78	2.65	2.68(2.57)	3.4
$\Gamma_{2'c}$	3.83	3.34	2.96	3.66(3.56)	4.2
X_{1v}	−7.75	−7.93	−7.96		
X_{4v}	−2.79	−2.90	−2.92		-2.9, -3.3 ± 0.2
X_{1c}	1.29	0.75	0.56		
E_g	1.15	0.62	0.43	0.66(0.52)	1.17

[a] Reference [12]. The LDA eigenvalues shown in parentheses are slightly different from our LDA values because of the difference in computational details.
[b] The experimental values are taken from reference [41] for Si.

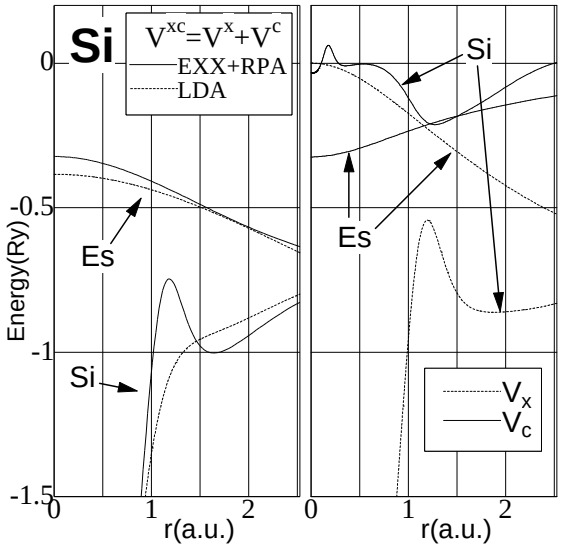

Figure 5. The exact exchange potential V^x and the RPA correlation potential V^c for Si. The LDA XC potential [28], used as the reference, is calculated for the density determined by the self-consistent calculation using the EXX + RPA. There exists an ambiguity in the constant shifts for V^x and V^c.

the difference in the computational method; their method used pseudopotentials and was not self-consistent but was free from the static approximation described in section 2 for W_p. In figure 5, we see that V^c cancels the large difference of V^x between Si and empty spheres.

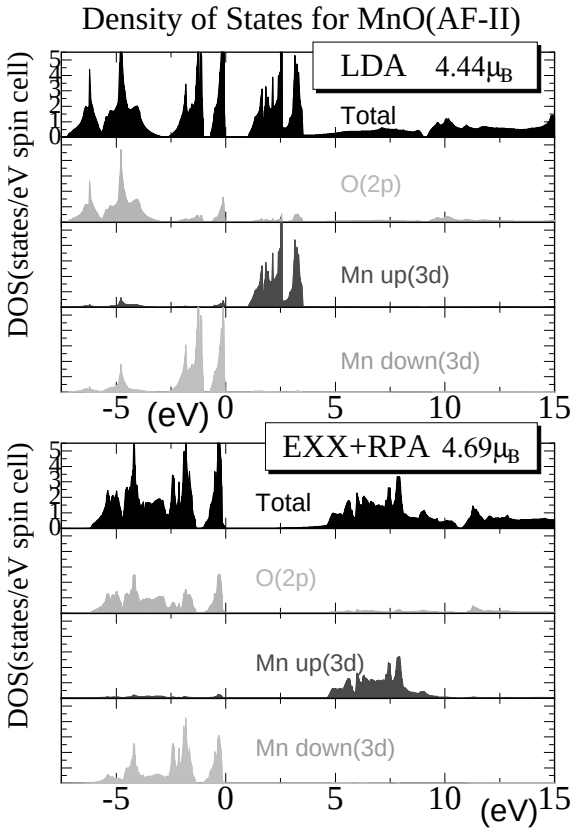

Figure 6. The DOS for MnO.

As a result, V^{xc} obtained using the EXX + RPA becomes very close to that obtained from the LDA.

We show the DOS of MnO in figure 6. To plot the eigenvalues of the unoccupied states for MnO precisely, we recalculate these values with $\epsilon_{\nu Rl}$, which are set to about the eigenvalue of the bottom of the conduction bands [24]. The results obtained by using the EXX + RPA are very different from those obtained using the LDA; the exchange splitting of Mn(3d), ≈8 eV, is much larger than the LDA value, ≈4 eV, and smaller than the EXX value, ≈13 eV [4]. The DOS shows good correspondence with the XPS + BIS data on MnO [13]. For such a system as MnO, with a large band gap, we cannot expect large screening effects like in metals. Therefore, it is reasonable that the EXX + RPA results lie in between the LDA and EXX results. We can see this point also from figure 7, where we show the self-consistent V^{xc}: the contribution of V^{x} is only partially cancelled by V^{c}, which is different from the case for metals.

In contrast to the LDA results, the tops of the valence bands obtained by using the EXX + RPA have large O(2p) components. The exchange effect, which works as an attractive force and was not correctly treated in the LDA, pushes down the localized occupied bands relative to the unoccupied bands. The effect is stronger for Mn(3d) bands than for O(2p) bands because Mn(3d) is more localized. Our method can give a reasonable screening effect for the exchange. It gives a good agreement with experiments as regards the DOS. The corresponding energy bands are shown in figure 8. The bottom of the conduction bands

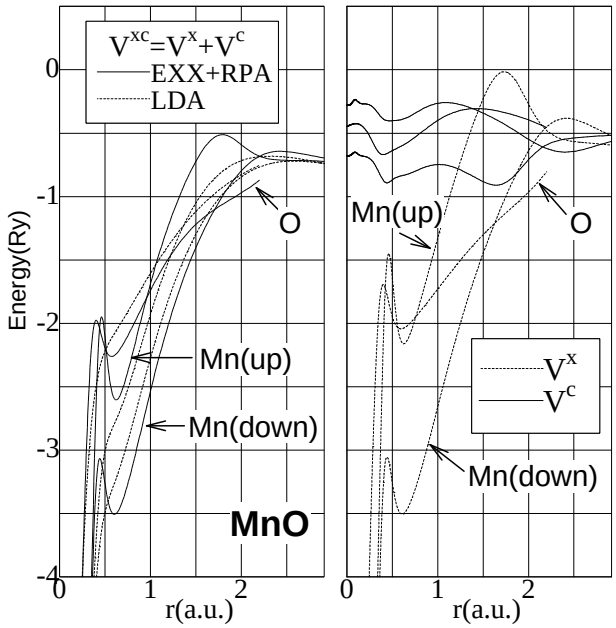

(a)

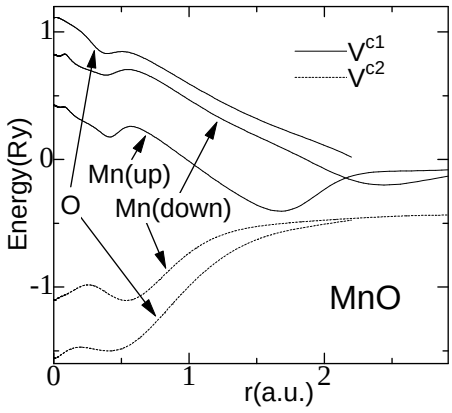

(b)

Figure 7. V^{xc} for MnO. In (b), we show the decomposition of $V^{xc} = V^{c1} + V^{c2}$.

is s-like, and the minimum gap of 2.3 eV obtained from the EXX + RPA is much larger than the LDA result, though it still is smaller than the experimental values of 3.7 ± 0.1 eV [32]. The spin magnetic moment of 4.69 μ_B gives a better agreement with the experiments (4.79 μ_B–4.58 μ_B [33, 34]).

In reference [26], for NiO it was shown that the GW-calculation with W_p based on the LDA eigenvalues gave poor results because of the LDA band gap being too small, and that self-consistency of GW was necessary. We can avoid this difficulty of the GW-calculation by use of the OEP method; we expect that the GW-approximation starting from the eigenvalues and eigenfunctions given by the EXX + RPA method will give reasonable agreement with experiments.

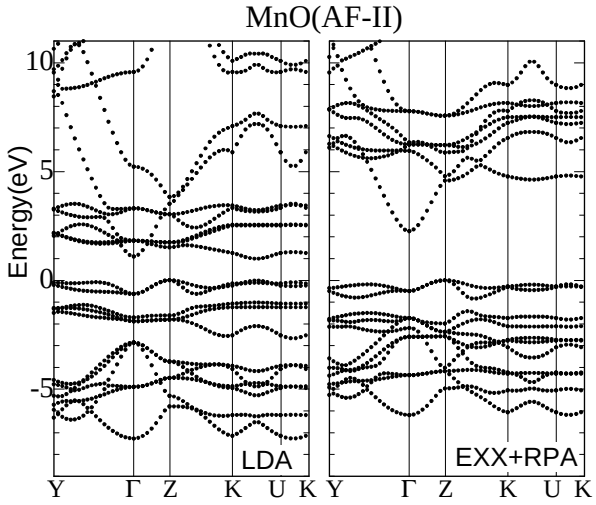

Figure 8. Energy bands for MnO.

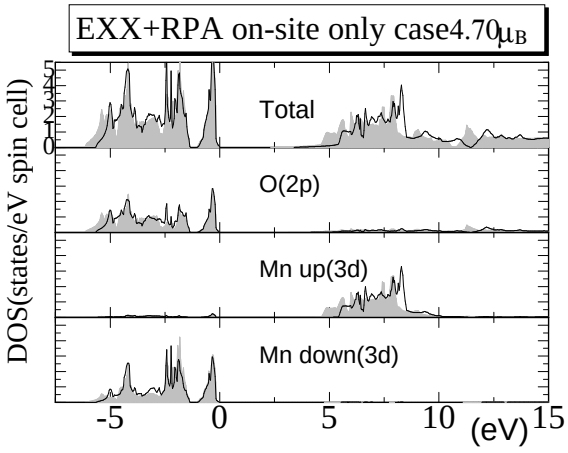

Figure 9. The DOS for MnO (the on-site-only case).

4.3. Further discussion

$E_{\rm xc}$ consists of all of the contributions from all of the pairs (R, R'). However, we can expect the contributions of $R \neq R'$ not to be large compared with the contribution of $R = R'$, and they might be negligible. In order to examine this point, we have performed an on-site-only EXX + RPA calculation, where we take only the $R = R'$ term into account. The difference from the full calculation is not so large for Fe; it gives a slightly larger moment, 2.10 $\mu_{\rm B}$. The bottom of the valence band (the bottom of the s bands) relative to the Fermi level is pushed up by ∼0.5 eV, though the d bands are essentially unchanged. On the other hand, the difference in the DOS from the full calculation is not so small in the case of MnO, as shown in figure 9. In this case, the on-site-only calculation gives narrower valence bands, and the conduction bands are pushed up by ∼1 eV, although the spin magnetic moment changes little (4.71 $\mu_{\rm B}$). In conclusion, the on-site-only approximation works, but the quality of the result depends on the systems and on the physical quantities which are calculated.

Let us discuss two possible sources of the existing differences between our results and those obtained using the true DF: (i) the RPA, and (ii) the static approximation for the RPA. In order to take account of the effects beyond the RPA, we have to treat $f_{\rm xc}$ given in reference [19], which corresponds to the vertex correction. Some parts of the contribution due to $f_{\rm xc}$ might be taken into account by LDA-like approximations; one of the simple ways to do this is to add the difference between the LDA XC calculated by using the RPA [28] and the one calculated by using a more accurate scheme [35]. We tried the above method, but the correction turned out to be rather small; the magnetization of Fe was enhanced by 0.05 $\mu_{\rm B}$ (this value is similar to that in the corresponding LDA case). However, we are not very confident about whether the correction is really meaningful or not. As for the static approximation for the RPA, the dynamical effects may be simulated by making $v_{\rm sc}^{\omega=0}$ closer to v (no relaxation limit). This should reduce the magnitude of $V^{\rm c}$. Therefore the position of the d bands relative to the s band should be somehow pushed down for the Cu case (see figure 2). This estimation concerning (ii) is opposite in the case of the LDA. In the case of the LDA, we can easily show that the d bands calculated by using the LDA in the RPA [28] are pushed up from those obtained by using its static approximation. In conclusion, it seems rather difficult to evaluate (ii) on the basis of a simple LDA-like idea; we have not yet succeeded in giving any reasonable evaluations for the magnitude of the errors due to (i) and (ii).

5. Summary

We have presented a new method for carrying out self-consistent electronic structure calculations, the OEP method with the EXX + RPA within the LMTO-ASA. The method determines not only $V^{\rm eff}$, but also $W_{\rm p}$ in a self-consistent manner. For Fe, Co, Ni, and Cu, the agreements with experiments as regards hyperfine interactions are improved from the LDA results, although the energy bands and the magnetic moments are very close to those obtained using the LDA. For Si, the minimum gap is only 0.19 eV larger than the LDA result. This is in reasonable agreement with the results from previous work [5]. On the other hand, the exchange splitting for MnO is much larger than the LDA result and in good agreement with experiments [13]. We expect that the GW-calculation starting from the eigenvalues self-consistently determined by the OEP method will give reasonable agreement with experiments. We have not developed the code to calculate $E_{\rm c}^{\rm RPA}$ itself yet. The static approximation in the evaluation of its functional derivative $\delta E_{\rm c}^{\rm RPA}/\delta n^{\rm s}$ cannot be applicable. We are now trying such calculations to determine lattice constants and other cohesive properties.

Acknowledgments

I thank F Aryasetiawan for his GW-program and for stimulating discussions, and M van Schilfgaarde, T A Paxton, O Jepsen, and O K Andersen for their TB-LMTO program. I also thank H Akai for discussions and for a critical reading of the manuscript.

Appendix A. Discontinuity of $V^{\rm xc}$ and the band gap

The inversion equation for obtaining $V^{\rm xc}(\boldsymbol{r}) \equiv \delta E_{\rm xc}/\delta n(\boldsymbol{r})$ is

$$\frac{\delta E_{\rm xc}}{\delta V^{\rm eff}(\boldsymbol{r})} = \int {\rm d}r' \, \frac{\delta n(\boldsymbol{r}')}{\delta V^{\rm eff}(\boldsymbol{r})} \frac{\delta E_{\rm xc}}{\delta n(\boldsymbol{r}')}. \tag{A1}$$

In the case of insulators with band gaps, we have a discontinuity in $V^{\rm xc}$. This comes from the differences between two limits: (a) $\mu \to \mu^+$ and (b) $\mu \to \mu^-$. We can easily show that

$$\frac{\delta E_{\rm xc}}{\delta V^{\rm eff}(\boldsymbol{r})} = \underline{\frac{\delta E_{\rm xc}}{\delta V^{\rm eff}(\boldsymbol{r})}} + \frac{\delta E_{\rm xc}}{\delta \mu}\frac{1}{\delta N/\delta \mu}\frac{\delta N}{\delta V^{\rm eff}(\boldsymbol{r})} \tag{A2}$$

$$\frac{\delta n(\boldsymbol{r}')}{\delta V^{\rm eff}(\boldsymbol{r})} = \underline{\frac{\delta n(\boldsymbol{r}')}{\delta V^{\rm eff}(\boldsymbol{r})}} + \frac{\delta n(\boldsymbol{r}')}{\delta \mu}\frac{1}{\delta N/\delta \mu}\frac{\delta N}{\delta V^{\rm eff}(\boldsymbol{r})} \tag{A3}$$

where only the second terms on the r.h.s. are dependent on the limits. The first terms (with underlines) are the quantities defined under the condition of fixed total numbers of electrons; their integrals with respect to $\boldsymbol{r}'$ are equal to zero. N denotes the total number of electrons per cell. $\delta/\delta\mu$ corresponds to the constant shift of $V^{\rm eff}(\boldsymbol{r})$. By substituting the solution of $V^{\rm xc} + C_\pm$ ($C_\pm$ denotes the constant part for each limit) for equation (A1), we can obtain two equations for determining $V^{\rm xc}$ and C:

$$\underline{\frac{\delta E_{\rm xc}}{\delta V^{\rm eff}(\boldsymbol{r})}} = \int {\rm d}r' \, \underline{\frac{\delta n(\boldsymbol{r}')}{\delta V^{\rm eff}(\boldsymbol{r})}} V^{\rm xc}(\boldsymbol{r}') \tag{A4}$$

$$\left(\frac{\delta E_{\rm xc}}{\delta \mu}\right)_\pm = \int {\rm d}r' \left(\frac{\delta n(\boldsymbol{r}')}{\delta \mu}\right)_\pm (V^{\rm xc}(\boldsymbol{r}') + C_\pm). \tag{A5}$$

Equation (A4) determines $V^{\rm xc}$ to within a constant. Apart from such a constant, $V^{\rm xc}$ is independent of the method of taking the limits (a) and (b). Equation (A5), which determines C, can be rewritten as

$$\Delta E_{\rm xc}\big|_\pm = \Delta V^{\rm xc}\big|_\pm + C_\pm \tag{A6}$$

where $\Delta E_{\rm xc}$ is the difference between two $E_{\rm xc}$s, one for adding and another for subtracting one electron by shifting μ in the state k, which corresponds to the lowest unoccupied state or the highest occupied state. It is equal to $\Sigma^{\rm RPA}(k, \epsilon_k)$. Therefore the discontinuity $\Delta_{\rm xc} \equiv C_+ - C_-$ can be written as

$$\Delta_{\rm xc} = (\Sigma^{\rm RPA}(k_+, \epsilon_{k_+}) - \langle k_+|V^{\rm xc}|k_+\rangle) - (\Sigma^{\rm RPA}(k_-, \epsilon_{k_-}) - \langle k_-|V^{\rm xc}|k_-\rangle) \tag{A7}$$

where we use $\Delta V^{\rm xc} = \langle k|V^{\rm xc}|k\rangle$. $\Delta_{\rm xc}$ agrees with the band gap which is calculated by using the GW-approximation. This equation is a generalization of the equation used in the evaluation of the discontinuity in reference [9].

References

[1] Talman J D and Shadwick W F 1976 *Phys. Rev.* A **14** 36
[2] Kotani T 1995 *Phys. Rev. Lett.* **74** 2989
Kotani T 1994 *Phys. Rev.* B **50** 14 816 (erratum 1995 **51** 13 903)
Kotani T and Akai H 1995 *Phys. Rev.* B **52** 17 153
[3] Kotani T and Akai H 1997 *Physica* B **237+238** 332
[4] Kotani T and Akai H 1996 *Phys. Rev.* B **54** 16 502
[5] Kotani T 1997 *Preprint* cond-mat/9711062
Kotani T and Akai H 1998 *J. Magn. Magn. Mater.* **177–181** 569
[6] Krieger J B, Li Y and Iafrate G J 1992 *Phys. Rev.* A **45** 101
[7] Li Y, Krieger J B and Iafrate G J 1993 *Phys. Rev.* A **47** 165
[8] Bylander D M and Kleinman L 1995 *Phys. Rev. Lett.* **74** 3660
Bylander D M and Kleinman L 1995 *Phys. Rev.* B **52** 14 566
[9] Städele M, Majewski J A, Vogl P and Göling A 1997 *Phys. Rev. Lett.* **79** 2089
[10] Aashamar K, Luke T M and Talman J D 1979 *J. Phys. B: At. Mol. Phys.* **12** 3455
[11] Aryasetiawan F and Gunnarsson O 1994 *Phys. Rev.* B **49** 16 214

[12] Godby R W, Shlüter M and Sham L J 1988 *Phys. Rev.* B **37** 10 159
[13] van Elp J, Potze R H, Eskes H, Berger R and Sawatzky G A 1991 *Phys. Rev.* B **44** 1530
[14] Luttinger J M and Ward J C 1960 *Phys. Rev.* **118** 1417
[15] Harris J and Jones R O 1974 *J. Phys. F: Met. Phys.* **4** 1170
[16] Langreth D C and Perdew J P 1975 *Solid State Commun.* **31** 1425
[17] Gunnarsson O and Lundqvist B I 1976 *Phys. Rev.* B **13** 4274
[18] Fukuda R, Kotani T, Suzuki Y and Yokojima S 1994 *Prog. Theor. Phys.* **92** 833
[19] Gross E K U, Dobson J F and Petersilka M 1996 *Density Functional Theory (Springer Topics in Current Chemistry 181)* ed R F Nalewajski (Berlin: Springer) p 81
[20] Hedin L and Lundqvist S 1969 *Solid State Physics* vol 23, ed H Ehrenreich, F Seitz and D Turnbull (New York: Academic) p 1
[21] Andersen O K, Jepsen O and Glötzel D 1985 *Highlights of Condensed-Matter Theory* ed F Bassani, F Fumi and M P Tosi (Amsterdam: North-Holland) p 59
[22] Andersen O K, Pawloska Z and Jepsen O 1986 *Phys. Rev.* B **34** 5253
[23] Svane A and Andersen O K 1986 *Phys. Rev.* B **34** 5512
[24] van Schilfgaarde M, Paxton T A, Jepsen O and Andersen O K 1992 *The TB-LMTO Program* version 4 (Max-Planck-Institut für Festkörperforschung)
[25] Aryasetiawan F 1992 *Phys. Rev.* B **46** 13 051
[26] Aryasetiawan F and Gunnarsson O 1995 *Phys. Rev. Lett.* **74** 3221
Aryasetiawan F and Karlsson K 1996 *Phys. Rev.* B **54** 5353
[27] Rath J and Freeman A J 1975 *Phys. Rev.* B **11** 2109
[28] The RPA level of the LDA, given by
von Barth U and Hedin L 1972 *J. Phys. C: Solid State Phys.* **5** 1629
[29] *American Institute of Physics Handbook* 1972 3rd edn (New York: AIP)
[30] Akai H, Akai M, Blügel S, Drittler B, Ebert H, Terakura K, Zeller R and Dedrichs P 1990 *Prog. Theor. Phys. Suppl.* **101** 11
[31] Battocletti M, Ebert H and Akai H 1996 *Phys. Rev.* B **53** 9776
[32] Iskenderov R N, Drabkin I A, Emel'yanova L T and Ksendzov Ya M 1969 *Sov. Phys.–Solid State* **10** 2031
[33] Fender B E F, Jacobson A J and Wegwood F A 1968 *J. Chem. Phys.* **48** 990
[34] Cheetham A K and Hope D A O 1983 *Phys. Rev.* B **27** 6964
[35] Vosko S H, Wilk L and Nusair M 1980 *Can. J. Phys.* **58** 1200
[36] Kanamori J 1963 *Prog. Theor. Phys.* **30** 275
[37] Kanamori J 1996 *Phys. Rev.* B **54** 13 566
[38] Springer M, Aryasetiawan F and Karlsson K 1998 *Phys. Rev. Lett.* **80** 2389
[39] Reck R A and Fry D J 1969 *Phys. Rev.* **184** 492
Denan H, Herr A and Meyer A J P 1968 *J. Appl. Phys.* **39** 69
Besnus M J, Meyer A J P and Berninger R 1970 *Phys. Lett.* **32A** 192
[40] Moruzzi V L, Janak J F and Williams A R 1971 *Calculated Electronic Properties of Metals* (New York: Pergamon)
[41] Hybertsen M S and Louie S G 1986 *Phys. Rev.* B **34** 5390